1 **How to use empirical data to improve transportation infrastructure**

2 **risk assessment**

3 *Weihua Zhu[1,2], Kai Liu [1, 2*], Ming Wang [1,2], Sadhana Nirandjan[3], Elco E. Koks[3]*

4 *[1] School of national security and emergency management, Beijing Normal University, Beijing*

5 *100875, China*

6 *[2] Academy of Disaster Reduction and Emergency Management, Faculty of Geographical Science,*

7 *Beijing Normal University, Beijing 100875, China*

8 *[3]Institute for Environmental Studies (IVM), Vrije Universiteit Amsterdam, 1081 HV Amsterdam,*

9 *The Netherlands*

10 *Correspondence to Kai Liu (liukai@bnu.edu.cn).*

11 **Abstract:**

12 Rainfall-induced hazards, such as landslides, debris flows, and floods cause significant

13 damage to transportation infrastructure. However, an accurate assessment of rainfall-induced

14 hazard risk to transportation infrastructure is limited by the lack of regional and asset-tailored

15 vulnerability curves. This study aims to use multi-source empirical damage data to generate

16 vulnerability curves and assess the risk of transportation infrastructure to rainfall-induced

17 hazards. The methodology is exemplified through a case study for the Chinese national railway

18 infrastructure. In doing so, regional and national-level vulnerability curves are derived based

19 on historical railway damage records. This is combined with daily precipitation data and the

20 railway infrastructure market value to estimate regional- and national-level risk. The results

21 show large variations in the shape of the vulnerability curves across the different regions. The

22 railway infrastructure in Northeast and Northwest China is more vulnerable to rainfall-induced

23 hazards due to low protection standards. The expected annual damage (EAD) ranges from 1.88

1   to 5.98 billion RMB for the Chinese railway infrastructure, with a mean value of 3.91 billion

2   RMB. However, the risk of railway infrastructure in China shows high spatial differences due

3   to the spatially uneven precipitation characteristics, exposure distribution, and vulnerability

4   curves. The South, East and Central provinces have a high risk to rainfall-induced hazards,

5   resulting in an average EAD of 184 million RMB, 176 and 156 million RMB, respectively,

6   whereas the risk in the Northeast and Northwest provinces are estimated to be relatively lower.

7   The usage of multi-source empirical data offer opportunities to perform risk assessments that

8   include spatial detail among regions. These risk assessments are highly needed in order to make

9   effective decisions to make our infrastructure resilient.

10   Keywords: multi-source empirical data, vulnerability curve, risk estimate, damage

11   length factor

1. Introduction

13   In recent years, extreme precipitation events have increased in both frequency and intensity

14   in the context of global warming (Shi et al., 2018; Cardoso Pereira et al., 2020; Li et al., 2020).

15   Extreme precipitation may generate landslides, debris flows, and floods, which have the

16   potential to damage transportation infrastructure and disrupt transportation functions, thereby

17   posing a severe threat to the economy and society (Pregnolato et al., 2017; Diakakis et al., 2020;

18   Petrova, 2020). In July 2021, Zhengzhou was hit by a heavy downpour, that reached a

19   cumulative precipitation of 617.1mm in three days. The associated flash floods resulted in the

20   destruction of the Zhengzhou metro system; suspension of more than 80 bus lines; damage to

21   67 urban bridges, culverts and tunnels; cancellation and delay of more than 200 flights from

1   Zhengzhou airport; and flooded lines, collapsed roadbeds, and waterlogging of equipment

2   forcing railway operators to shut down for several days (Fig. 1a). On May 23, 2010, a landslide

3   occurred in the Yujiang-Dongxiang section of the Shanghai-Kunming Railway in Jiangxi

4   Province, causing the derailment of passenger train K859 (Fig. 1b). The sliding body was 60

5   metres long, 30 metres wide, and 3-8 metres thick, resulting in a volume of approximately 9,000

6   cubic metres. The cumulative precipitation in the 11 days before the incident was 251.5 mm in

7   Xiaogang town, Dongxiang County. In China, the average annual direct damage of railway

8   infrastructure caused by rainfall-induced hazards was approximately 3.29 billion RMB from

9   2000 to 2017 and has increased in recent years (Editorial Board of China Railway Yearbook,

10   2001-2017).
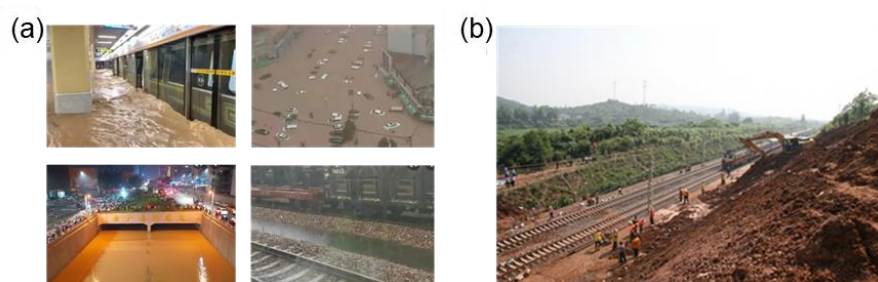
11

12   Fig. 1 (a) Transportation infrastructure damaged by floods triggered by extreme precipitation

13   at Zhengzhou, Henan province (2021); (b) Railroad damage by a debris flow triggered by

14   extreme precipitation at Xiaogang, Jiangxi Province (2010).

15   Accurate assessment of transportation infrastructure damage and risk due to hazards

16   triggered by rainfall is an essential component in transportation infrastructure risk management

17   (Liu et al., 2018a, 2021). In general, transportation infrastructure impacts due to natural hazards

18   include two aspects: (1) direct damage to the structure (Koseki et al., 2012; Kellermann et al.,

19   2015; Koks et al., 2019); and (2) indirect impact to the transportation service and associated

1   macroeconomic impact (Lamb et al., 2019). Determining direct damage is commonly done

2   using vulnerability curves (Englhardt et al., 2019; Koks et al., 2019), which typically present

3   the damage degree of infrastructure assets that would occur at specific hazard intensities

4   (Jongman et al., 2012; Ward et al., 2013). As the critical link of hazard characteristics and

5   damage loss, few studies (e.g. Sande and C.J, 2001; Kok et al., 2004; Huizinga et al., 2017)

6   tried to work on vulnerability curves for transportation infrastructure assets in different regions.

7   In these studies, empirical and synthetic approaches are usually adopted to develop curves

8   based on damage data (Merz et al., 2010) and expert judgement (Gerl et al., 2016).

9   Unfortunately, due to the lack of detailed damage data, such damage curves are unavailable for

10 most regions. Habermann and Hedel (2018) conducted a literature review on the damage

11 functions for transportation infrastructure due to wildfires and floods. They found that damage

12 functions for the transportation sector are scarce in the literature, and damage curves for the

13 transportation sector in different publications vary in shapes and values.

14   This article aims to use multi-source empirical damage data to assess the vulnerability and

15 risk of transportation infrastructure associated with rainfall-induced hazards (i.e. landslides,

16 debris flows, and floods). We develop a first set of regional and national vulnerability curves

17 for Chinese railway infrastructure that relates the damage degree of railway assets to

18 precipitation intensities. Based on these vulnerability curves, the risk of the railway

19 infrastructure associated with rainfall-induced hazards is estimated.

20   The remainder of the article is organized as follows. Section 2 describes this work's datasets,

21 including data on precipitation, historical railway damage, yearly railway damage and railway

1   market value. Section 3 describes the methodological framework, thereby elaborating on the

2   method for: (1) vulnerability assessment, (2) and risk estimation. Section 4 presents the main

3   results. Sections 5 and 6 discuss the results and conclude the article.

4   **2. Data collection**

5   **2.1 Precipitation data**

6   The CN05.1 dataset provides information on the observed daily precipitation from 1961 to

7   2018 at a 0.25 °spatial resolution (Wu and Gao, 2013; Zhang et al., 2019). The dataset is derived

8   from more than 2,400 in situ gauging stations by the Chinese Meteorological Administration

9   (CMA). The CN05.1 product has been recognized to be more reliable than its previous versions

10   because of the inclusion of more ground stations (Yatagai et al., 2009; Zhang et al., 2019). The

11   resolution of the CN05.1, however, is too coarse to accurately capture local extreme

12   precipitation events. As a complementary precipitation dataset, we therefore extract local

13   precipitation information from multiple news sources for 37% of the damage records (see

14   section 2.2). These news sources contain precipitation data obtained from rain gauges installed

15   by the railway department, thus measuring local extreme precipitation.

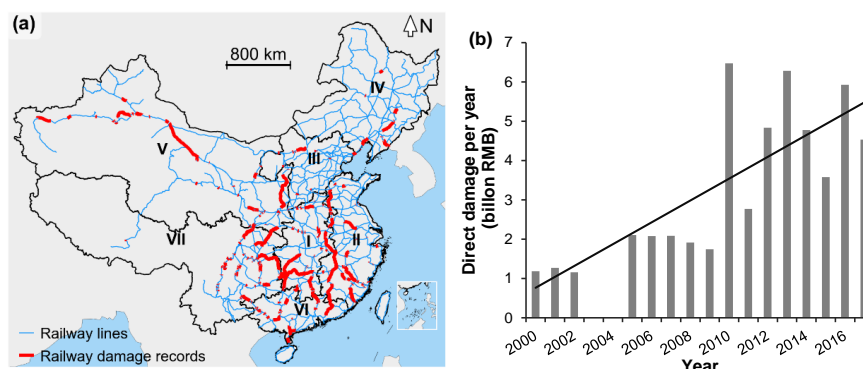## 2.2 Historical railway damage by rainfall-induced hazards

Fig. 2 (a) Spatial distribution of national railway damage records. We divide the mainland of
China into seven geographical divisions: Central China (I), East China (II), North China (III),
Northeast China (IV), Northwest China (V), South China (VI), and Southwest China (VII).
(b) Temporal distribution of historical damage to the national railway infrastructure by
rainfall-induced hazards from 2000 to 2016. Railway geometries © OpenStreetMap
contributors 2019. Distributed under the Open Data Commons Open Database License
(ODbL) v1.0.

Zhao et al. (2020) catalogued 464 railway disasters caused by rainfall-induced hazards in the

Chinese railway system between 2000 and 2016. After removing service disruption disasters

(i.e. trains that slow down or stop for safety reasons) that are irrelevant for this study, we found

a total of 236 railway damage records that represent structural damage to railway assets or

debris covering the rail. The spatial distribution of the filtered set of national railway damage

records is presented in Fig. 2a. For all these records, we collect information about the

occurrence date of the damage, the damage location, and the descriptive damage state by using

online publicly available news sources. In this study, if damages induced by a precipitation

event occurred in the segment between two adjacent stations, one damage record is counted.

1 Table 1 gives some typical railway damage records over 1981–2016. The information of the all

2 damage records used in this study can be found in supplement material.

3 Table 1 Typical railway damage records over 1981–2016.

Damage date	Url	Railway name	Damag segment	Damage state
2005/6/21	http://news.sina.com.cn/c/2005-06-25/10586266797s.shtml	Yingxia railway	Panfang-Yangkou	Geological, severe
2005/6/21	http://news.sina.com.cn/c/2005-06-25/10586266797s.shtml	Yingxia railway	Xiawangtang-Shaikou	Geological, severe
2013/7/13	http://www.eeb.cn/tabid/372/infoid/1521/frtid/89/default.aspx	Baoxi railway	Yanan-Yananbei	Embankment, Moderate
2016/7/17	https://baike.so.com/doc/24425372-25257771.html	Jiaoliu railway	Wanyan-Longbizui	Track, severe

4 For the available 236 railway damage records, 84% occurred in the summer (June, July, and

5 August). Most of the disasters occurred in July, accounting for 40% of the 236 railway damage

6 records; 30% and 14% occurred in June and August, respectively. These numbers correspond

7 to most parts of China's rainy seasons in which precipitation is a crucial trigger of rainfall-

8 induced hazards. Fig. 2a shows the spatial distribution of railway damage for the years 2000-

9 2016. The results show that the national railway lines suffered widespread rainfall-induced

10 damage, especially in South China. Detailed spatial distributions of damages and associated

11 reasons were explored in previous research of Liu et al.(2018) and Zhao et al. (2020). To explore

12 the spatial distribution of railway vulnerability in different regions, China was divided into

13 seven sub-regions based on seven geographical divisions (Liu et al., 2020), as shown in Fig. 2a:

14 Central China (I), East China (II), North China (III), Northeast China (IV), Northwest China

1   (V), South China (VI), and Southwest China (VII) (Liu et al., 2020).

2.3 Railway damage yearly data

Two datasets are used to obtain railway damage yearly data: the national railway yearbooks (Editorial Board of China Railway Yearbook, 2001-2017) and the Zhengzhou regional administrator's yearbooks (Editorial Board of Zhengzhou Administrator's Railway Yearbook, 2001-2017). The national railway yearbooks cover data on the direct damage, total damage length and the number of total damage events (one damage event is defined as a main railway line is damaged by a precipitation event) per year for the national railway system. The Zhengzhou regional administrator's yearbooks provide information on the number of total damage events and the total number of damaged places (i.e. a continuous section of damage) per year for the Zhengzhou administrator railway system (ZHR), from 2000 to 2017 by rainfall-induced hazards.

An overview of the yearly railway damage obtained from the two sources is shown in Table 2. Fig. 2b shows the direct damage per year from 2000 to 2017 (missing data in 2003 and 2004); the economic damage significantly increased from 2000 to 2017, which is due to the increased railway exposure and extreme precipitation events (Zhao et al., 2020). The average annual economic damage is estimated to be 3.29 billion RMB. The ZHR damage data shows that each damage event causes multiple damage places on railway infrastructure, with an average of nine damage places per event. Assuming that the number is the same for the national railway system, we calculate that the average damage length is 753 m per damage place for an event using the total number of damage events and total damage length at a national level.

Natural Hazards
and Earth System
Sciences
Discussions
Open Access
EGU

1   Table 2 Railway damage for the period 2000-2017

Year	National			Zhengzhou Administrator	
	Damage event times	Damage length (km)	Direct damage (billon)	Damage event times	Damage places
2000	183	478.6	1.179		
2001	98	358.8	1.266	42	469
2002	106	441.1	1.156	21	174
2003	142			81	125
2004	122			114	224
2005	203		2.105	36	169
2006	128	922.8	2.073	34	170
2007	121	832.6	2.081	40	247
2008	75	802.1	1.911	7	272
2009	86	511.1	1.741	17	226
2010	177	1066.6	6.473	20	354
2011	109	1107.0	2.767	8	144
2012	99	1606.0	4.833	41	160
2013	113	709.0	6.280	65	144
2014	82	654.0	4.774	52	206
2015	91	265.0	3.576	37	90
2016	211	388.0	5.923	53	246
2017	165	488.0	4.531	37	205

2   **2.4 Railway market value**

3   The railway market value is from the World Bank Office, China (Gerald Ollivier, 2014).

4   They provide the range of average unit costs for the 200 km/h double-track railway (AUC-

5   200D) shown in Table 3. The AUC-200D divides the cost of the railway into five elements, (1)

1   land acquisition and resettlement, and four first-level structures: (2) civil works (embankment,

2   bridge or trunk), (3) track, (4) signalling, and (5) communications and electrifications. We use

3   the mean value to present the unit cost of the element (e.g. the mean value is 6 million/per km

4   of track element). The average railway market value used in this work is 56 million RMB,

5   which does not consider land acquisition and resettlement costs since those parts were paid

6   before construction.

7   Table 3 Range of average unit costs (RMB million/per km of double track)

Element		RMB million/per km of double track		Average unit costs (RMB million/per km of double track)
Land acquisition and resettlement		5-8		6.5
Civil Works	Embankment	23-28	42-43	42.5
	Bridges/viaducts	59-62		
	Tunnels	51-68		
Track (ballasted)		5-7		6
Signalling and communications		3-4		3.5
Electrification		4		4

8   **3. Methods**

9   Figure 3 presents an overview of the methodological framework used in this study. The

10   methods in this study are divided into two parts: (1) vulnerability assessment and (2) risk

11   estimation. In the first part, national and regional vulnerability curves that characterize the

12   railway susceptibility by relating the damage degree to precipitation intensity are generated. In

1   the second part of the research, we estimate the risk to the Chinese railway system. The railway

2   market value is combined with the vulnerability curve developed in the first part of the research

3   and spatial data on the precipitation intensity to calculate the risk represented by expected

4   annual damage (EAD).

5
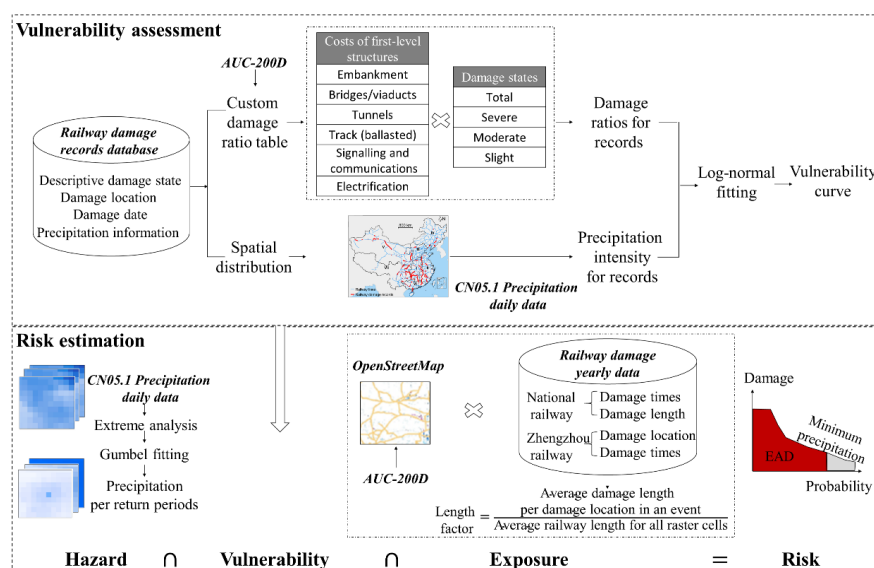
6   Fig. 3 Methodology of using the multiple sources of data to estimate vulnerability and risk.

7   Railway geometries © OpenStreetMap contributors 2019. Distributed under the Open Data

8   Commons Open Database License (ODbL) v1.0.

9   **3.1 Vulnerability curve estimation**

10   **3.1.1 Precipitation intensity estimated for damage records**

11   The 88 damage records that are provided with additional local precipitation information from

12   the news are shown in Fig. 4a with red lines. For each remaining damage record, we use the

13   maximum 1-day precipitation amount along the damaged segment in the five consecutive days

14   (M1-5d) before the damage occurred to present the precipitation intensity, shown in Fig. 4a

1   with black lines. To keep the consistency of the precipitation, we use the extracted precipitation

2   information from the news to correct the M1-5d. The relationship between precipitation from

3   news and M1-5d is given in Eq. (1) and derived using a least-squares fitting method, as

4   presented in Fig. 4b, with R square 0.63. The constructed curve allows us to transform the

5   precipitation in CN05.1($pre(CN05.1)$) to the local precipitation as far as possible.

6    $$pre(news) = 1.87 * pre(CN05.1) + 27.35 \qquad (1)$$
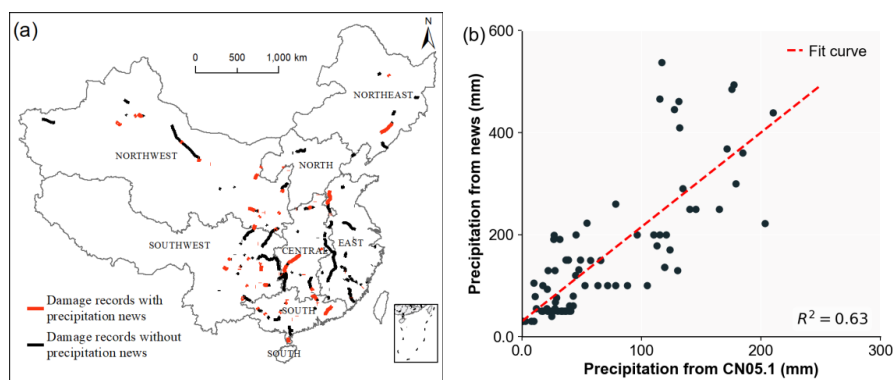

7

8   Fig. 4 (a) Spatial distribution of precipitation extracted from news and CN05.1; (b) The

9   relationship between precipitation extracted from news and CN05.1.

10   **3.1.2 Calculation of the damage ratio**

11   The damage ratio is the ratio of the cost of repairing to the cost of rebuilding (Mazzorana et

12   al., 2009), which is estimated by the news information and AUC-200D. First, we generate a

13   custom damage ratio table based on the AUC-200D and the descriptive damage state is given

14   in Sections 2.2 and 2.4. Second, we transform the descriptive damage state into a numerical

15   damage ratio using the damage ratio table. There are three steps that we use to build the custom

16   damage ratio table:

1. Determine the cost ratio of the railway value for first-level structures. Based on AUC-200D in Table 3, we calculate the cost ratio among four first-level structures. Taking the civil works: embankment as an example, the 'total cost' ratio is 0.65, 0.25, 0.09, 0.1 for embankment track, signalling, communications and electrifications, respectively. For bridges and tunnels, the total cost ratios are shown in Appendix Table A2.

2. Classify the damage state for each first-level structure and give the numerical damage ratio range for each classification. The final damage states and the associated numerical ratio are divided into four classifications, namely, total damage (1), severe damage (0.66-0.99), moderate damage (0.33-0.66), and light damage (0.01-0.33), as shown in Table 4.

3. Calculate the numerical damage ratio range for a combination of a railway structure and a damaged state, and determine associated damage descriptive information based on news sources for each combination. The final damage ratio table is presented in Table 4, which is multiplied by the cost ratio of a first-level structure and the range ratio of the damage state classification. We then classify the damage state in sec 2.2 into each category.

Based on the damage ratio table and the historical news, we obtain the numerical damage ratio for each record. For each event, three damage ratios, namely, minimum ratio, average ratio, and maximum ratio, are obtained based on the damage ratio range. For example, the minimum ratio for the embankment's severe damage state is 0.644, and the average and maximum ratios

1   are 0.536 and 0.429, respectively.

2   Table 4 Damage ratio table

Element	Unit cost ratio	Damage state	Damage ratio	Description
Embankment	0.6500	Total	0.6500	Total damage
		Severe	0.4290-0.6435	Suspended sleepers; Hanging rails
		Moderate	0.2145-0.4290	Subgrade shoulder, drainage ditch, side drain, revetment slope protection, protecting wall: moderate damage, collapse
		Slight	0.0065-0.2145	Subgrade shoulder, drainage ditch, side drain, revetment slope protection, protecting wall: mild damage, cracks, blockage, loose, wash out
Track	0.1500	Total	0.1500	Total damage
		Severe	0.0990-0.1485	Near-failure of components: sleepers, rail, track bed
		Moderate	0.0495-0.0990	Two-component failure: sleepers, rail, track bed
		Slight	0.0015-0.4950	Single-component failure: sleepers, rail, track bed
Signalling and communications	0.0900	Total	0.0900	Total damage
		Severe	0.0594-0.0891	Near-destruction of components: digital tuning and TDCS equipment
		Moderate	0.0297-0.0594	One-component destruction: digital tuning and TDCS equipment

		Slight	0.0009-0.0297	Communication equipment interrupted
		Total	0.1000	Total damage
Electrification	0.1000	Severe	0.0660-0.0990	Power supply equipment damage and Catenary pillar destruction
		Moderate	0.0330-0.0660	Power supply equipment damage
		Light	0.0010-0.0330	Catenary pillar destruction

3.1.3 Fitting the vulnerability curves

We choose the log-normal distribution to fit the vulnerability curve. The cumulative

distribution function of log-normal distribution is shown in Eq. 2,

$$P(x) = \emptyset[\frac{\ln(x/\varphi)}{\xi}] \tag{2}$$

which has two parameters, the location parameter φ and the scale parameter ξ, namely, the

median and standard values, respectively (Porter et al., 2007). We use the precipitation intensity

as the x value and the damage ratio as the $P(x)$ value. A log-normal vulnerability function is

chosen because it is a parsimonious two-parameter distribution with positive support (ensuring

that unrealistic negative loads cannot occur) and has many precedents for its use in fragility

analysis (Porter et al., 2007).

In this study, we generate a total of seven vulnerability curves for the railway system: one

for each of the six sub-regions (we combine North China into Central China since the damage

records are less in North China), and one at the national level. To eliminate the noise and

significant changes in the damage ratio, a moving average method is used to smooth the damage

ratio in each precipitation intensity range. We use the criteria for classifying the precipitation

intensity issued by the China Meteorological Administrator (2008), which is presented in Table

1   5, to apply the moving average method.

2   Table 5 Classification of the precipitation intensity

Precipitation intensity	Total precipitation, in 24 h/mm
Light rain	0.1-9.9
Light rain-Moderate rain	5.0-16.9
Moderate rain	10.0-24.9
Moderate rain-Heavy rain	17.0-37.9
Heavy rain	25.0-49.9
Heavy rain-Torrential rain	33.0-74.9
Torrential rain	50.0-99.9
Torrential rain-Downpour	75.0-174.9
Downpour	100.0-249.9
Downpour-Heavy downpour	175.0-299.9
Heavy downpour	≥ 250.0

3   **3.2 Risk assessment**

4   To calculate the direct risk to the Chinese railway infrastructure, we develop precipitation

5   maps for different return periods based on the Gumbel distribution. From the daily precipitation

6   time series in the CN05.1 product (1961-2018), we extract an annual time series of maximum

7   precipitation volumes for 1961-2018. For each cell, we then fit a Gumbel distribution

8   (Nadarajah, 2010) through this time series based on non-zero data. These Gumbel parameters

9   are used to calculate precipitation volumes per grid cell for selected return periods (2, 5, 10, 25,

10   50, 100, 200, 250, 500, and 1000 years). Precipitation volumes are calculated conditionally on

11   the exceedance probability of zero precipitation volume. For those cells where less than five

12   non-zero data points are available, the precipitation volume is assumed to be zero (Ward et al.,

1   2013).

2   Risk is generally calculated by combining the hazard intensity, vulnerability, and exposure

3   (Merz et al., 2009; Lamb et al., 2019). In this study, we present risk as expected annual damage

4   (EAD) (Merz et al., 2009). The EAD is defined as the average expected yearly market loss and

5   is estimated based on selected discrete hazard events with different return periods. The EAD is

6   calculated using the trapezoidal rule (Espinet et al., 2018). The EAD of the Chinese railway

7   system is expressed in Eq. 5 as follows:

8
$$\text{EAD} = \frac{1}{2}\sum_{r=1}^{n}\left(\frac{1}{T_r} - \frac{1}{T_{r+1}}\right)(D_i + D_{r+1}) \tag{3}$$

9   where T_r is the rth return period, D_i is associated with damage to the railway

10   infrastructure, which is defined in Eqs. (4) and (5) :

11
$$D_i = \sum_{i}^{N} H_r^i * V * E_i * C_{\text{DL}} \tag{4}$$

12
$$C_{\text{DL}} = \frac{DL}{L} \tag{5}$$

13   where H_r^i is the precipitation intensity amount of raster cell i with a return period of

14   T- year, V is the vulnerability curve, E_i is the railway market value of raster cell i, N is the

15   number of raster cells that intersect the railway line, and C_{DL} is a damage length factor for

16   calibration. In Eq. 5, DL is the average damage length (753 m) per damage place in an event,

17   and L is the average railway length for all raster cells that intersect with railway lines. This

18   study and previous studies assume that assets exposed in one raster cell are exposed to the same

19   damage degree for a certain hazard intensity. Based on the yearly railway damage data (sec 2.3),

20   the average damage length in one damage place per event is 753 m. This is much shorter

21   compared to the precipitation resolution (ca. 28 km) used in this work and is also shorter than

22   the average railway length in each cell (ca. 14.6 km for double-track lines). We, therefore,

1   introduce a damage length factor (C_{DL}) to calibrate the estimated damage, assuming that not

2   the entire railway section in a specific cell suffers damage from an event.

3   **4. Results**

4   **4.1 Vulnerability curves**

5   The national- and regional-level vulnerability curves are presented in Fig. 5. The upper

6   boundary is the maximum vulnerability curve, the lower boundary is the minimum vulnerability

7   curve, and the middle black line is the average vulnerability curve, fitted by maximum,

8   minimum, and average ratios, respectively. Vulnerability curves have noticeable regional

9   differences across the country. When considering relatively low precipitation intensities,

10   railway lines in Northwest China are vulnerable to rainfall-induced hazards. Damage ratios in

11   Northwest China are higher than other regional- and national-level damage ratios with the same

12   precipitation intensity. For example, when the precipitation is 100 mm (torrential rain), the

13   national railway damage ratio is 0.124, whereas the railway damage ratio in Northwest China

14   is about 0.148. Railway lines in Northwest and Northeast China are particularly vulnerable to

15   rainfall events with high precipitation intensities. In case of extensive precipitation of more than

16   200 mm (downpour), the national railway damage ratio is approximately 0.175, the railway

17   damage ratio in Northeast China is about 0.180, and the railway damage ratio in Northwest

18   China can reach 0.212. In Northwest China, the precipitation amount over 100 years is less than

19   100 mm. Considering the low frequency of extreme precipitation and the expensive cost of high

20   protection standards, the Northwest China railway infrastructures are not robust relative to other

21   areas when looking at the same precipitation. In Northeast China, the oldest railway lines, which

Natural Hazards
and Earth System
Sciences
Discussions

1   have not been updated, have relatively low design standards and inadequate drainage facilities

2   to defend against extreme precipitation, resulting in higher vulnerabilities compared to other

3   regions.
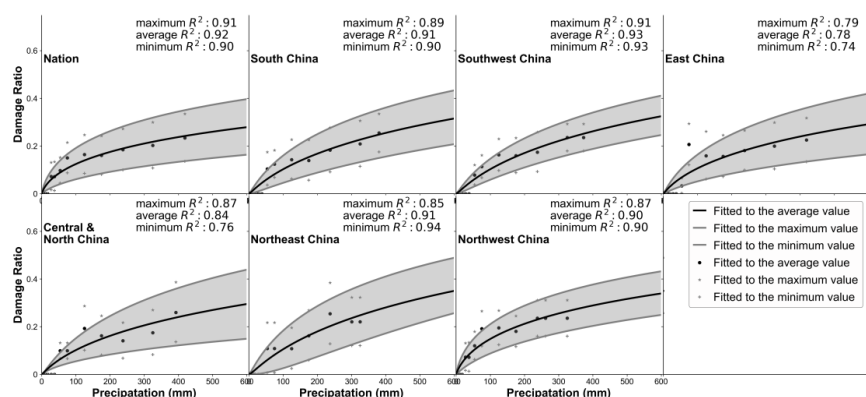
5   Fig. 5 National and regional vulnerability curves between precipitation (mm) and damage

6   ratio. The maximum R^2 is the R square for the maximum vulnerability curve, the average

7   R^2 is the R square for the average vulnerability curve, the minimum R^2 is the R square for

8   the minimum vulnerability curve.

9   **4.2 Risk analysis**

10   To incorporate the regional characteristics of the vulnerability for the Chinese railway system,

11   we use the regional vulnerability curves to assess the risk of the Chinese railway system. We

12   calculated the annual direct damage to railway infrastructure from 2000 to 2017, of which the

13   results are presented in Fig. 6. The grey area is the range of annual direct damage, with the

14   upper boundary calculated based on the maximum vulnerability curve, the lower boundary

15   calculated based on the minimum vulnerability curve, and the middle darker grey line

16   calculated based on the average vulnerability curve, thereby using the regional vulnerability

17   curves. The darker yellow dots are the annual statistical damage in the yearbook with a 10%

19

1   error scale. Compared to the statistical damage, we find that estimated damage is

2   underestimated for high annual damage and overestimated for small annual damage, which is

3   a consequence of using mean damage ratios for each precipitation range in the vulnerability

4   curves. Damage in 2000, 2001 and 2002 is overestimated, and the estimated damage is

5   calculated with the minimum vulnerability with 38%, 15% and 22% deviation from the

6   statistical damage. For the left, 81.25% of the statistically damaged points are located in the

7   estimated damage range. These results illustrate that the fitted vulnerability curves can be used

8   to calculate the damage.

9
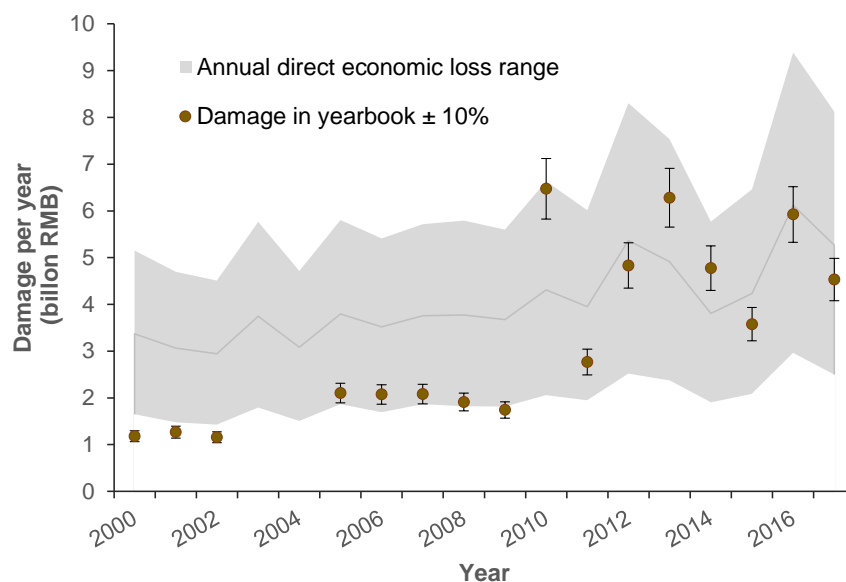
10

11   Fig. 6 Annual direct damage due to damage to railway infrastructure from 2000 to 2017 in

12   China.

13   The regional and national EAD to railway infrastructure due to rainfall-induced hazards are

14   presented in Fig. 7 using regional vulnerability curves. The national railway EAD is

1   approximately 3.91 billion RMB when calculated with average vulnerability curves. When

2   calculated with minimum and maximum vulnerability curves, the national EAD is 1.88 billion

3   RMB and 5.98 billion RMB, respectively. Regionally, damage among areas differs substantially.

4   Using the results calculated with average vulnerability as an example, East China has the

5   highest risk with approximately 1.0 billion RMB, which exceeds the national EAD with 25.5%.

6   North, South and Southwest China face a similar risk, with approximately 15%, 14%, and 13%

7   of total national damage, respectively. High-density railway infrastructure exposure combined

8   with a high frequency of extreme precipitation in these regions results in railway infrastructure

9   with the highest risk.

10
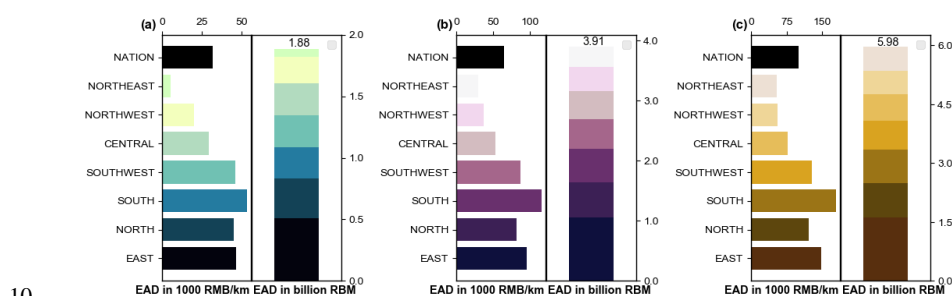
11   Fig. 7 Rainfall-induced hazard risk per region using different vulnerability curves. (a) The

12   minimum vulnerability curve; (b) The average vulnerability curve; (c) The maximum

13   vulnerability curve. The numbers on top of each stacked column chart are the national EAD

14   values using the different vulnerability curves.

15   The national EAD per kilometre ranges from 32 to 86 thousand RMB, with an average of

16   65.38 thousand RMB using the average vulnerability curve. The EAD per kilometre is the

17   highest in South China using the average vulnerability curves, which is 116.11 thousand RMB,

18   followed by East China and Southwest China, for which the numbers are 96.30 and 87.37

19   thousand RMB, respectively. The railways in South, East and Southwest China require much

1   attention and must improve their robustness.

2   The risk per province calculated using the regional average vulnerability curves of the

3   railway infrastructure to the rainfall-induced hazards are presented in Fig. 8. The risk differs

4   considerably between regions when expressed in total EAD and EAD per kilometre. An

5   examination of the total EAD shows that the provinces in North China, such as Hebei, Shanxi,

6   Shandong, Henan, Southwest Sichuan and South Guangdong, experience the highest risks and

7   is estimated to be larger than 200 million RMB. Hebei, Shandong have the most extended

8   infrastructure assets in China. The railway in Shanxi and Sichuan are vulnerable to rainfall-

9   induced hazards, as shown in Fig. 5. When looking at EAD per kilometre for each province,

10 the provinces in Southwest China, such as Sichuan and coastal provinces(e.g. Guangdong,

11 Fujian, and Hainan), have the highest risks. The total EAD and EAD per kilometre are high in

12 Sichuan, Shanxi and Guangdong provinces. From the provincial perspective, these two

13 provinces need to allocate more resources to reduce the risk of rainfall-induced hazards.

14
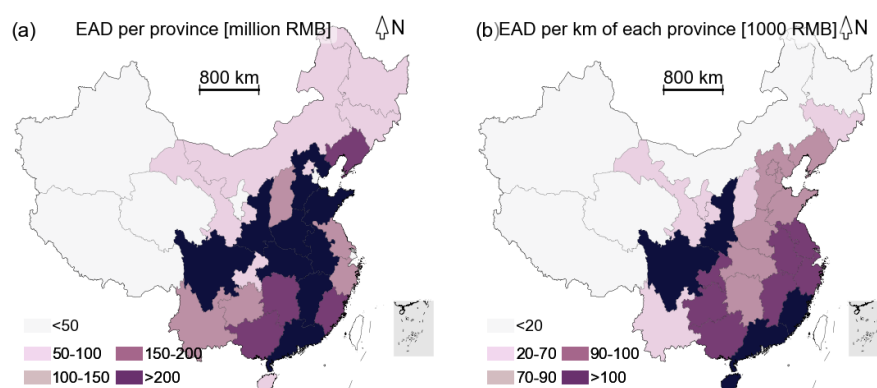
15 Fig. 8 Rainfall-induced hazard risk per province using the average vulnerability curve (a)

16 EAD per province (million RMB) and (b) EAD per km of each province (1000 RMB). Fig.

17 A.1 provides a map of provinces of China.

5. Discussion

This study uses multi-source empirical data to assess the vulnerability and risk to railway infrastructure in China associated with rainfall-induced hazards. For this purpose, the damage news information and a custom damage ratio table are used to fit regional and national vulnerability curves. Previous studies (e.g. Quan Luna et al., 2011; Papathoma-Köhle et al., 2012; Silva and Pereira, 2014; Stephenson and D'Ayala, 2014; Tsubaki et al., 2016; Pregnolato et al., 2017) have tried to use empirical data to fit the fragility or vulnerability curves to hazard intensity and object damage ratio in some regions. In these studies, detailed photos (Papathoma-Köhle et al., 2012; Pregnolato et al., 2017) or hazard model results (Quan Luna et al., 2011) are mostly used to drive the hazard intensity, and adequate documentation of the damage and reconstruction cost can be used to calculate damage ratios. Due to the strict requirement of spatiotemporal damage and hazard intensity information, regional and national vulnerability curves to link hazard characteristics and exposures are rare in many regions. This work tries to overcome the universal problem of the lack of detailed vulnerability data. The fitted vulnerability curves are used as the descriptive damage state in the information on damage and precipitation derived from the news and exited precipitation dataset; these data are more easily collected. Combining the fitted vulnerability curve, precipitation product, and railway infrastructure exposure, the estimated risk of the national railway infrastructure, after calibration with a damage length factor, is approximately 3.91 billion RMB. The overall railway infrastructure risk results are broadly correlated with the yearbook average direct economic damage from 2000 to 2017, which is 3.29 billion RMB. The results reveal that vulnerability

23

1   and risk can be estimated accurately using multi-source empirical data.

2   Several assumptions and limitations are acknowledged in this study. First, for damage

3   records without local precipitation information, we use the maximum daily precipitation 5 days

4   before damage occurrence (M1-5d) along the damaged segment to present the precipitation

5   intensity. However, there exists deviation for the local damage places along with the damaged

6   segments. In addition, the resolution of the CN05.1 precipitation data is too coarse to accurately

7   capture local extreme precipitation events. We hence use the extracted precipitation information

8   from the news to correct the M1-5d. In a certain way, it would decrease the uncertainty and

9   keep the consistency of the precipitation. Second, due to a lack of different railway market

10   values and detailed information on each railway infrastructure, this work uses the railway

11   market value for 200 km/h railways of double tracks as the value for all types of railway

12   infrastructure. This leads to an overestimation of risk because most conventional railway speeds

13   are lower than 200 km/h, and the relative price has a high probability of being lower than 56

14   million RMB. Post-disaster reconstruction using higher design standards to improve railways'

15   ability to defend against disasters can reduce the risk for future hazards.

16   From approximate and common news information to national datasets (e.g. railway damage

17   data), the method used in this work can be a new direction to assess vulnerability and risk by

18   combining multiple sources of empirical data. In addition, the low resolution of the

19   spatiotemporal hazard map smooths the extreme values and cannot capture the hazardous

20   damage. Future research needs to develop a high-resolution spatiotemporal hazard map to

21   prevent this issue.

6. Conclusion

In this study, we use multi-source empirical data to assess the vulnerability and risk to railway infrastructure in China associated with rainfall-induced hazards. Regional- and national-level precipitation vulnerability curves are derived based on news information and a custom damage ratio table. Based on precipitation data, fitted vulnerability curves, the market value of railway infrastructure, and a damage length factor, we assess and calibrate the annual direct damage from 2000 to 2017 caused by rainfall-induced hazards to Chinese railway infrastructure.

Due to the spatial unevenness of protection standards, the regional vulnerability curves of railway infrastructure to rainfall-induced hazards show high spatial inconsistency. Railways in South, Southwest, North, East, and Central China are robust to rainfall-induced hazards since higher protection standards have been used to defend the heaviest rainfall. Railways in Northwest and Northwest China are relatively vulnerable to rainfall-induced hazards. In addition, the regional curves generated in this study can be applied in other works after adjusting the length factor based on the methodology illustrated in sec 3.2.

The national railway infrastructure risk is approximately 3.91 billion RMB, and we find that the estimated annual direct damage of railway infrastructure to rainfall-induced hazards increases due to increasing extreme precipitation and railway exposure. Due to the spatially uneven precipitation intensity, exposure distribution and vulnerability curves, the risk in China show high spatial differences. The heaviest rainfall and high exposure density lead to a high absolute risk to railway infrastructure in South, East and Southwest China, even though they are robust to rainfall-induced hazards. Provinces such as Sichuan and Guangdong have high

1 absolute and relative risks. For railway infrastructure risk reduction and sustainable

2 development of railway transportation in China, more attention and high protection standards

3 need to be allocated to these high-risk areas. This work provides regional and national

4 vulnerability and risk information for decision-makers.

Code/Data availability

6 Supporting data are accessible through the associated reference, and the historical railway

7 damage data used is in supplement material. The data in this study were analysed with Python

8 package, and the figures were created with ArcViewTM GIS and Python packages. All codes

9 used in this work are available upon request.

Author contribution

11 Kai Liu and Weihua Zhu developed the original idea and designed the analyses. Elco Koks

12 contributed to the study design. Weihua Zhu and Kai Liu conducted the analysis. Weihua Zhu

13 wrote the original manuscript, and Kai Liu, Ming Wang, Sadhana Nirandjan and Elco Koks

14 provided comments and revised the manuscript. All the co-authors contributed to scientific

15 interpretations of the results.

Declaration of Competing Interest

17 The authors declare that they have no known competing financial interests or personal

18 relationships that could have appeared to influence the work reported in this paper.

Acknowledgements

Natural Hazards
and Earth System
Sciences
Discussions

4   **Reference**

5   Cardoso Pereira, S., Marta-Almeida, M., Carvalho, A. C. and Rocha, A.: Extreme precipitation

6   events under climate change in the Iberian Peninsula, Int. J. Climatol., 40(2), 1255–1278,

7   doi:10.1002/joc.6269, 2020.

8   Diakakis, M., Boufidis, N., Salanova Grau, J. M., Andreadakis, E. and Stamos, I.: A systematic

9   assessment of the effects of extreme flash floods on transportation infrastructure and circulation:

10 The example of the 2017 Mandra flood, Int. J. Disaster Risk Reduct., 47(February), 101542,

11 doi:10.1016/j.ijdrr.2020.101542, 2020.

12 Editorial Board of China Railway Yearbook, Ed.: China railway yearbook, China Railway

13 Publishing House, Beijing., 2001.

14 Editorial Board of China Railway Yearbook, Ed.: China railway yearbook, China Railway

15 Publishing House, Beijing., 2009.

16 Englhardt, J., De Moel, H., Huyck, C. K., De Ruiter, M. C., Aerts, J. C. J. H. and Ward, P. J.:

17 Enhancement of large-scale flood risk assessments using building-material-based vulnerability

18 curves for an object-based approach in urban and rural areas, Nat. Hazards Earth Syst. Sci.,

19 19(8), 1703–1722, doi:10.5194/nhess-19-1703-2019, 2019.

20 Espinet, X., Rozenberg, J., Ogita, K. S. R. S., Singh Rao, K. and Ogita, S.: Piloting the Use of

21 Network Analysis and Decision-Making under Uncertainty in Transport Operations:

22 Preparation and Appraisal of a Rural Roads Project in Mozambique Under Changing Flood

23 Risk and Other Deep Uncertainties., 2018.

24 Gerald Ollivier, J. S. and N. Z.: High-Speed Railways in China: A Look at Construction Costs.,

25 2014.

26 Habermann, N. and Hedel, R.: Damage functions for transport infrastructure, Int. J. Disaster

27 Resil. Built Environ., 9(4–5), 420–434, doi:10.1108/IJDRBE-09-2017-0052, 2018.

Natural Hazards
and Earth System
Sciences
Open Access
Discussions
EGU

1   Huizinga, J., de Moel, H. and Szewczyk, W.: Global flood depth-damage functions :

2   Methodology and the Database with Guidelines., 2017.

3   Jia, W. and Xuejie, G.: A gridded daily observation dataset over China region and comparison

4   with the other datasets, Chinese J. Geophys., 56(4), 1102–1111, 2013.

5   Jongman, B., Kreibich, H., Apel, H., Barredo, J. I., Bates, P. D., Feyen, L., Gericke, A., Neal,

6   J., Aerts, J. C. J. H. and Ward, P. J.: Comparative flood damage model assessment: Towards a

7   European approach, Nat. Hazards Earth Syst. Sci., 12(12), 3733–3752, doi:10.5194/nhess-12-

8   3733-2012, 2012.

9   Kellermann, P., Schöbel, A., Kundela, G. and Thieken, A. H.: Estimating flood damage to

10 railway infrastructure - The case study of the March River flood in 2006 at the Austrian

11 Northern Railway, Nat. Hazards Earth Syst. Sci., 15(11), 2485–2496, doi:10.5194/nhess-15-

12 2485-2015, 2015.

13 Kok, M., Huizinga, H., Vrouwenfelder, A. and Berendregt, A.: Damage and casualties caused

14 by flooding, 2004.

15 Koks, E. E., Rozenberg, J., Zorn, C., Tariverdi, M., Vousdoukas, M., Fraser, S. A., Hall, J. W.

16 and Hallegatte, S.: A global multi-hazard risk analysis of road and railway infrastructure assets,

17 Nat. Commun., 10(1), 1–12, doi:10.1038/s41467-019-10442-3, 2019.

18 Lamb, R., Garside, P., Pant, R. and Hall, J. W.: A Probabilistic Model of the Economic Risk to

19 Britain's Railway Network from Bridge Scour During Floods, Risk Anal.,

20 doi:10.1111/risa.13370, 2019.

21 Li, L., Zou, Y., Li, Y., Lin, H., Liu, D. L., Wang, B., Yao, N. and Song, S.: Trends, change

22 points and spatial variability in extreme precipitation events from 1961 to 2017 in China,

23 Hydrol. Res., 51(3), 484–504, doi:10.2166/nh.2020.095, 2020.

24 Liu, K., Wang, M., Cao, Y., Zhu, W., Wu, J. and Yan, X.: A comprehensive risk analysis of

25 transportation networks affected by rainfall-Induced multihazards, Risk Anal., 38(8), 1618–

26 1633, doi:10.1111/risa.12968, 2018a.

27 Liu, K., Wang, M., Cao, Y., Zhu, W. and Yang, G.: Susceptibility of existing and planned

28 Chinese railway system subjected to rainfall-induced multi-hazards, Transp. Res. Part A Policy

Natural Hazards
and Earth System
Sciences
Discussions

Open Access

EGU

1   Pract., 117, 214–226, 2018b.

2   Liu, K., Wang, M. and Zhou, T.: Increasing costs to Chinese railway infrastructure by extreme

3   precipitation in a warmer world, Transp. Res. Part D Transp. Environ., 93(March),

4   doi:10.1016/j.trd.2021.102797, 2021.

5   Liu, W., Wu, J., Tang, R., Ye, M. and Yang, J.: Daily precipitation threshold for rainstorm and

6   flood disaster in the mainland of China: An economic loss perspective, Sustain., 12(1),

7   doi:10.3390/SU12010407, 2020.

8   Nadarajah, S.: The exponentiated Gumbel distribution with climate application, Environmetrics,

9   17(1), 13–23, 2010.

10   Papathoma-Köhle, M., Keiler, M., Totschnig, R. and Glade, T.: Improvement of vulnerability

11   curves using data from extreme events: Debris flow event in South Tyrol, Nat. Hazards, 64(3),

12   2083–2105, doi:10.1007/s11069-012-0105-9, 2012.

13   Petrova, E.: Natural hazard impacts on transport infrastructure in Russia, Nat. Hazards Earth

14   Syst. Sci., 20(7), 1969–1983, doi:10.5194/nhess-20-1969-2020, 2020.

15   Pregnolato, M., Ford, A., Wilkinson, S. M. and Dawson, R. J.: The impact of flooding on road

16   transport: A depth-disruption function, Transp. Res. Part D Transp. Environ., 55, 67–81,

17   doi:10.1016/j.trd.2017.06.020, 2017.

18   Quan Luna, B., Blahut, J., Van Westen, C. J., Sterlacchini, S., Van Asch, T. W. J. and Akbas,

19   S. O.: The application of numerical debris flow modelling for the generation of physical

20   vulnerability curves, Nat. Hazards Earth Syst. Sci., 11(7), 2047–2060, doi:10.5194/nhess-11-

21   2047-2011, 2011.

22   Sande, van der and C.J: River flood damage assessment using IKONOS imagery, Eur. Comm.

23   Jt. Res. Centre, Nat. Hazards Unit – Floods, Ispra (Va), ItalyEuropean Comm. Jt. Res. Centre,

24   Nat. Hazards Unit – Floods, Ispra (Va), Italy, (January 2001), 2001.

25   Shi, J., Cui, L., Wen, K., Tian, Z., Wei, P. and Zhang, B.: Trends in the consecutive days of

26   temperature and precipitation extremes in China during 1961–2015, Environ. Res., 161(July

27   2017), 381–391, doi:10.1016/j.envres.2017.11.037, 2018.

28   Silva, M. and Pereira, S.: Assessment of physical vulnerability and potential losses of buildings

1   due to shallow slides, Nat. Hazards, 72(2), 1029–1050, doi:10.1007/s11069-014-1052-4, 2014.

2   Stephenson, V. and D'Ayala, D.: A new approach to flood vulnerability assessment for historic

3   buildings in England, Nat. Hazards Earth Syst. Sci., 14(5), 1035–1048, doi:10.5194/nhess-14-

4   1035-2014, 2014.

5   Tsubaki, R., David Bricker, J., Ichii, K. and Kawahara, Y.: Development of fragility curves for

6   railway embankment and ballast scour due to overtopping flood flow, Nat. Hazards Earth Syst.

7   Sci., 16(12), 2455–2472, doi:10.5194/nhess-16-2455-2016, 2016.

8   Ward, P. J., Jongman, B., Weiland, F. S., Bouwman, A., Van Beek, R., Bierkens, M. F. P.,

9   Ligtvoet, W. and Winsemius, H. C.: Assessing flood risk at the global scale: Model setup,

10 results, and sensitivity, Environ. Res. Lett., 8(4), doi:10.1088/1748-9326/8/4/044019, 2013.

11 Yatagai, A., Arakawa, O., Kamiguchi, K., Kawamoto, H., Nodzu, M. I. and Hamada, A.: A 44-

12 year daily gridded precipitation dataset for Asia based on a dense network of rain gauges, Sci.

13 Online Lett. Atmos., 5(1), 137–140, doi:10.2151/sola.2009-035, 2009.

14 Zhang, X., Su, Z., Lv, J., Liu, W., Ma, M., Peng, J. and Leng, G.: A set of satellite-based near

15 real-time meteorological drought monitoring data over China, Remote Sens., 11(4), 1–12,

16 doi:10.3390/rs11040453, 2019.

17 Zhao, J., Liu, K. and Wang, M.: Exposure analysis of Chinese railways to multihazards based

18 on datasets from 2000 to 2016, Geomatics, Nat. Hazards Risk, 11(1), 272–287,

19 doi:10.1080/19475705.2020.1714753, 2020.

20

21

Natural Hazards
and Earth System
Sciences
Discussions

1   **Appendix**

3   Fig. A.1 Map showing the distribution of Chinese provinces. The China Provincial Map layer

4   comes from the Data Center for Resources and Environmental Sciences, Chinese Academy of

5   Sciences, which is accessible from the Resource and Environment Data Cloud Platform

6   (http://www.resdc.cn/, last access: 19 May 2020).

7   Table A1 (a) Damage ratio table

Element	Unit cost ratio	Damage state	Damage ratio	Description
Bridges/viaducts	0.8176	Total	0.8176	Total damage
		Severe	0.5396-0.8094	Almost components destruction: superstructure, bearing substructure and accessory structure damage
		Moderate	0.2698-0.5396	Two-components destruction: superstructure, bearing substructure and accessory structure damage

Element	Unit cost ratio	Damage state	Damage ratio	Description
		Slight	0.0082-0.2698	One-component destruction: superstructure, bearing substructure and accessory structure damage
Track	0.0811	Total	0.0811	Total damage
		Severe	0.0535-0.0803	Near-failure of components: sleepers, rail, trackbed
		Moderate	0.0268-0.0535	Two-component failure: sleepers, rail, trackbed
		Slight	0.0008-0.0268	Single-component failure: sleepers, rail, trackbed
Signalling and communications	0.0473	Total	0.0473	Total damage
		Severe	0.0312-0.0468	Near-destruction of components: digital tuning and TDCS equipment
		Moderate	0.156-0.0312	One-component destruction: digital tuning and TDCS equipment
		Slight	0.0005-0.0156	Communication equipment interrupted
Electrification	0.0540	Total	0.0541	Total damage
		Severe	0.0357-0.0535	Power supply equipment damage and Catenary pillar destruction
		Moderate	0.0178-0.0357	Power supply equipment damage
		Light	0.0005-0.0178	Catenary pillar destruction

1

2   Table A1 (b) Damage ratio table

Element	Unit cost ratio	Damage state	Damage ratio	Description
Tunnels	0.8095	Total	0. 8095	Total damage
		Severe	0.5379-0.8069	Almost components destruction: the

				slope, portal, lining of portal and lining, road or invert, surrounding rock of Tube
		Moderate	0.2690-0.5379	Two of third of components destruction: the slope, portal, lining of portal and lining, road or invert, surrounding rock of Tube
		Slight	0.0082-0.2690	One of third of component destruction: the slope, portal, Lining of portal and lining, road or invert, surrounding rock of Tube
Track	0.0794	Total	0.0822	Total damage
		Severe	0.0542-0.0814	Near-failure of components: sleepers, rail, track bed
		Moderate	0.0271-0.0542	Two-component failure: sleepers, rail, track bed
		Slight	0.0008-0.0271	Single-component failure: sleepers, rail, track bed
Signalling and communications	0.0476	Total	0.0479	Total damage
		Severe	0.0316-0.0475	Near-destruction of components: digital tuning and TDCS equipment
		Moderate	0.0158-0.0316	One-component destruction: digital tuning and TDCS equipment
		Slight	0.0005-0.0158	Communication equipment interrupted
Electrification	0.0635	Total	0.0548	Total damage
		Severe	0.0362-0.0542	Power supply equipment damage and Catenary pillar destruction
		Moderate	0.0181-0.0362	Power supply equipment damage

		Light	0.0005-0.0181	Catenary pillar destruction

1